

Shear viscosity of the Lennard-Jones fluid near the triple point: Green-Kubo results

Jerome J. Erpenbeck

Los Alamos National Laboratory, University of California, Los Alamos, New Mexico 87545

(Received 11 July 1988)

The long-standing disagreement over the shear viscosity coefficient of the Lennard-Jones fluid near the triple point is reexamined through a series of very extensive Monte Carlo molecular-dynamics calculations of this transport coefficient based on the Green-Kubo theory. The stress autocorrelation function is shown to exhibit a slow decay, principally in the kinetic-potential and the potential-potential terms, which is large compared with the kinetic-kinetic long-time tail predicted by simple mode-coupling theory. Nonetheless, the viscosity coefficient, exclusive of any correction for this tail for times greater than are accessible numerically, is found to agree with that of Schoen and Hoheisel (who discounted the existence of such a tail) as well as nonequilibrium molecular-dynamics calculations. The large value of the viscosity coefficient found by Levesque and co-workers for 864 particles is brought into statistical agreement with the present results by a modest, but not unrealistic, increase in its statistical uncertainty. The pressure is found to exhibit an anomalous dependence on the size of the system, but the viscosity as well as the self-diffusion constant appear to be linear in the inverse of the number of particles, within the precision of our calculations. The viscosity coefficient, including a long-time-tail contribution based on the extended mode-coupling theory is $(3.796 \pm 0.068)\sigma(\epsilon/m)^{1/2}$ for the Lennard-Jones potential, fitted to a cubic spline, and $(3.345 \pm 0.068)\sigma(\epsilon/m)^{1/2}$ for the potential truncated at 2.5σ .

I. INTRODUCTION

The Lennard-Jones (LJ) fluid has been studied over a broad range of temperature and densities using the numerical methods of statistical mechanics—Monte Carlo and molecular dynamics. While rather extensive calculations of the equation of state have been made, transport coefficients have been evaluated in far less detail, at least in part because of the relative difficulty of these calculations.

One particular state point, near the triple point, has acquired special importance with regard to transport properties, because it was chosen as a point of comparison between Green-Kubo (GK) and nonequilibrium molecular-dynamics (NEMD) calculations. The former include the equilibrium molecular-dynamics calculation by Levesque, Verlet, and K urkijarvi¹ which, at least by 1973 standards, was very extensive by virtue of the relatively large number of particles, $N=864$, and the length of the trajectory, 100 800 time steps. As a result, with the advent of NEMD it was regarded as the standard by which to compare other calculations, at least for nonsingular potentials.

When used to study shear viscosity, NEMD refers to a series of methods, originating in the early 1970s in the work of Hoover and Ashurst,^{2,3} Gosling, McDonald, and Singer,⁴ and Lees and Edwards.⁵ These calculations aimed to obtain the viscosity coefficient by subjecting the fluid to nonequilibrium boundary conditions, somewhat in the manner of a laboratory experiment, but using the computer to follow the development of the "flow" by solving the N -body equations of motion. However, spatial inhomogeneity and system heating made these calculations difficult to analyze for the transport coefficients.

Methods have more recently been developed to over-

come these obstacles. Hoover, Evans, and co-workers^{6,7} have generalized the early Lees-Edwards⁵ calculation for the shear viscosity through the use of non-Hamiltonian equations of motion, including the imposition of the constraint of constant temperature. While a number of distinct methods have been suggested and while these methods do not yield results which agree in all cases, nonetheless at high densities and in the limit of vanishing shear rate, the methods appear to yield indistinguishable results.

In the interest of establishing the efficacy of NEMD, at least in the limit of vanishing shear rate, a number of studies have been made of the shear viscosity coefficient of the triple-point LJ fluid. The aim of these studies was to ascertain that NEMD yielded correct values for the shear viscosity coefficient and did so more efficiently than other numerical methods. Two sources for comparison have been used, namely, the experimental value for argon and the GK calculations, including the Levesque, Verlet, and K urkijarvi study referred to above.

In the Hoover *et al.*⁶ comparison two facts were reported: (1) The NEMD result, which was reported to be independent of the number of particles in the system, was in good agreement with the experimental argon value; and (2) the NEMD results seems to differ sharply with the GK estimates, which included the $N=864$ results of Levesque, Verlet, and K urkijarvi,¹ in addition to the results of Levesque and Verlet⁸ for $N=108, 256,$ and 864 and of E. L. Pollock for 256 and 500 particles. (The latter have not been otherwise published.) If, however, one considers only the $N \leq 500$ results, then there appears to be essentially no disagreement. That is, if the two $N=864$ results of Levesque and co-workers^{1,8} could be dismissed as outliers, the problem would vanish.

Schoen and Hoheisel⁹ took note of the discrepancy in

their study of the shear viscosity of the Lennard-Jones fluid. They studied the behavior of the GK value for the viscosity coefficient, considering both the dependence on the size of the system (studying systems of 32 to 2048 particles) and on the extent of the GK time integral which formally extends to infinity. While there appears to be a number of inconsistencies in their results, they report a final estimate for the triple-point state which is in excellent agreement with the NEMD result.

Finally, Levesque and Verlet⁸ returned to the question in the publication of the calculations reported by Hoover *et al.*⁶ Taking cognizance of the Schoen-Hoheisel⁹ study, they attempted to isolate the source of the discrepancy by extending the earlier calculation in a number of ways so as to appraise the accuracy of the GK estimates. The reported results include values for 108, 256, and 864 particles, as well as results for the so-called WCA potential (LJ potential truncated at its minimum) for systems up to 4000 particles. Because their new 864-particle result agreed rather well with the Levesque-Verlet-Kürkijarvi¹ value, they were unable to resolve the mysterious discrepancy but concluded that their 864-particle system was in some sort of a long-lived glassy state. One particularly germane item which emerged in this paper was the fact that the “new” 864-particle calculation was actually an extension of the earlier one to 139 000 time steps, rather than a completely independent trajectory, as had previously appeared to be the case.

The existence of a long-lived state, as proposed by Levesque and Verlet, appears rather unlikely for at least two reasons. First, the density under study is that of a liquid and the number of particles in the system is relatively large. A metastable state has not been observed in any of the other calculations thus far reported, even for smaller systems. Second, the equation of state found for the 864-particle system is in fact that of the liquid, which argues that the trajectory has adequately sampled phase space.

Inasmuch as the extant $N=864$ result has not been incorporated into a coherent picture of the triple-point LJ viscosity, it seems clear that a serious discrepancy remains. Moreover, from the point of view of the GK results, the N dependence of the viscosity coefficient generally, and particularly the contribution from a possible long-time tail of the autocorrelation function, have not been addressed adequately.

It is our purpose to shed further light on this disagreement by undertaking an extensive GK calculation of the viscosity coefficient η . In particular, we attempt a complete characterization of the dependence of η on the number of particles N . In addition to the contributions considered by Levesque and Verlet,⁸ we have also taken special care to assess the limit for the long-time contribution to the GK result arising from the so-called long-time tail of the stress autocorrelation function.

In an extensive study of the viscosity of the hard-sphere fluid at high density, Erpenbeck and Wood¹⁰ concluded that it was not possible to accurately assess the long-time-tail contribution without further theoretical explanation of the observed stress autocorrelation function, which did not appear to agree with the predictions of the

mode-coupling theory.^{11–14} Now, however, Kirkpatrick,¹⁵ van Beijeren,¹⁶ and de Schepper *et al.*¹⁷ have made notable progress in the necessary theoretical extensions through extended mode-coupling theory. We estimate a long-time correction based on this theory, even though our method is somewhat *ad hoc*.

Finally, it is important to take cognizance of the anomalous N dependence of the equation of state which has been found for hard disks,¹⁸ hard spheres,^{10,19} and the LJ fluid²⁰ at similar high densities. Moreover, a high-density LJ system at a temperature well above the triple point was found to exhibit a similar anomaly in the N dependence of the self-diffusion constant.²⁰ In both cases (equation of state and self-diffusion), a nonmonotonic dependence on system size was observed, the effect of which was to limit the $1/N$ linear extrapolation to values of N larger than 500. Schoen and Hoheisel⁹ studied larger (as well as smaller) systems and within their statistical uncertainties observed no similar anomaly. In fact, except for systems of 32, 108, and 256 particles, they could find no dependence of the viscosity on the system size. Indeed, their $N=32$ system, which would be expected to exhibit unusual equilibrium and nonequilibrium properties because the cutoff distance for their interaction potential was much greater than half the length of the (periodic) unit cell, yielded a viscosity which fit well with the results for larger systems.

The present calculations are similar in spirit to the earlier ones. However, in addition to being rather more extensive, we concentrate on the accurate appraisal of the statistical uncertainty of the results. This is particularly straightforward for the present calculations which employ averaging over the canonical ensemble through the Monte Carlo method in addition to extensive time averaging over individual trajectories. While we find good agreement of our results with most of the previous work, we find a very serious, large discrepancy with a 256-particle result of Pollock in addition to a sizeable discrepancy with the 864-particle result of Levesque and Verlet. While the former is inexplicable in the absence of publication of any detail of the calculation, the latter can be ascribed to a rather modest underestimation of its statistical uncertainty.

Finally, the present calculations include results for both the usual LJ potential, truncated at 2.5σ , as well as very extensive calculations for the cubic-spline modification of the LJ potential introduced by Holian and Evans.²¹ For the present state, we find that the spline version introduces a 14% increase in the viscosity coefficient, at least to a first approximation independent of the value of N . The existence of such a significant change would tend to indicate that the effect of truncation of the LJ potential may also be quite significant. Therefore, the apparent agreement between the (truncated) LJ result and the experimental argon value could be somewhat misleading.

II. THEORY AND METHODS

While the calculations reported here are generally familiar, it is important that the details of the present con-

tribution be made clear. As a result, we recite the necessary details in this section.

A. System

The system consists of N interacting particles, each of mass m , contained in volume V at temperature T . The particles interact through a pairwise-additive central potential $\phi(r)$. We designate the positions and velocities of the particles by $r^N = \{\bar{r}_1, \dots, \bar{r}_N\}$ and $v^N = \{\bar{v}_1, \dots, \bar{v}_N\}$. A point in phase space is specified by $x^N = \{r^N, v^N\}$, so that a complete trajectory is given by $x^N(t)$.

In the present calculations, we chose a Lennard-Jones interaction potential, modified with a cubic spline,²¹

$$\phi(r) = \begin{cases} u(r) & \text{if } r \leq r_c \\ a(r - r_m)^2 + b(r - r_m)^3 & \text{if } r_c < r \leq r_m \\ 0 & \text{if } r_m < r \end{cases} \quad (1)$$

where $u(r)$ is the Lennard-Jones potential,

$$u(r) = 4\epsilon \left[\left(\frac{\sigma}{r} \right)^{12} - \left(\frac{\sigma}{r} \right)^6 \right]. \quad (2)$$

The crossover distance r_c is defined to be the point of maximum attraction,

$$r_c = (\frac{26}{7})^{1/6} \sigma, \quad (3)$$

of the LJ potential. The parameters a , b , and r_m of the cubic spline are defined by requiring that $\phi(r)$ and its first and second derivatives be continuous at r_c , whence

$$\begin{aligned} r_c - r_m &= 3u_0/2u_1 \\ &= u_1/(r_c - r_m) \\ &= -u_1/3(r_c - r_m)^2, \end{aligned} \quad (4)$$

in which u_n is the n th derivative of the LJ potential $u(r)$ at $r = r_c$.

While our modification of the LJ potential has been used in a number of studies, previous work on the viscosity of the LJ fluid has, for the most part, used an LJ potential truncated at a fixed cutoff of 2.5σ , beyond which the potential is taken to be zero. While this difference in the potential does not appear to lead to any qualitative difference in results, it does have important quantitative effects which will be discussed further. Some results for the truncated potential will also be presented in order to demonstrate these differences.

At least from the point of view of numerical calculations, the potential including the cubic spline seems preferable to the truncated potential in that the discontinuity in the interatomic force is thereby eliminated, which seems to be advantageous in minimizing the truncation error in the numerical integration. Moreover, for the cubic-spline modified LJ potential, there are no "truncation" corrections. On the other hand, no attempt has been made to calibrate the cubic-spline-modified LJ potential as an effective potential for various monoatomic systems, as has been done for the full LJ potential.

The system is subject to periodic boundary conditions,

so as to minimize the effects of the finite size of the system. Thus, the potential energy $\Phi(r^N)$ of the system contains contributions from the various "images" of the primary cell,

$$\begin{aligned} \Phi(r^N) &= \sum_{\vec{v}} \Phi_{\vec{v}}(r^N), \\ \Phi_{\vec{v}}(r^N) &= \sum'_{i,j \geq i} \phi(|\bar{r}_{ij} + \vec{v}L|), \\ \bar{r}_{ij} &= \bar{r}_i - \bar{r}_j, \end{aligned} \quad (5)$$

where the \vec{v} sum is over all three-vectors \vec{v} of signed integers. The system is cubic with length L so that $L^3 = V$. The prime on i, j sum indicates that the $i = j$ term is to be omitted for $\vec{v} = 0$.

B. Ensemble: Thermodynamic properties

The present calculations differ in another important respect from those discussed in Sec. I. Typically those calculations obtain observations of quantities of interest as time averages over a single trajectory of the system. Because energy and momentum are conserved, the latter observations are regarded as equivalent to averages in the so-called "molecular-dynamics ensemble," i.e., the submicrocanonical ensemble characterized by zero total momentum. Here, however, the standard Metropolis Monte Carlo method is used so that our estimates are for the canonical ensemble.

To obtain the thermodynamic pressure p we use the virial equation of state,

$$\frac{pV}{Nk_B T} = 1 - \frac{\langle W_N \rangle}{\langle E_k \rangle}, \quad (6)$$

in which k_B is the Boltzmann constant, W_N is the virial,

$$W_N = -\frac{1}{2} \sum_{\vec{v}} \sum'_{i,j \geq 1} (\bar{r}_{ij} + \vec{v}L) \cdot \bar{F}(\bar{r}_{ij} + \vec{v}L), \quad (7)$$

E_k is the kinetic energy, and the angular brackets denote the canonical ensemble average. Finally, $\bar{F}(\vec{r}) = -d\phi(\vec{r})/d\vec{r}$ is the force. The average kinetic energy in the canonical ensemble yields the temperature,

$$\langle E_k \rangle = 3Nk_B T/2, \quad (8)$$

but it is not necessarily advantageous to use this exact result in numerical calculations.

C. Green-Kubo theory

The GK formula for the shear viscosity coefficient is conveniently written as a sum of kinetic, potential, and cross terms,

$$\eta = \eta^{KK} + 2\eta^{K\phi} + \eta^{\phi\phi}, \quad (9)$$

where

$$\begin{aligned} \eta^{AB} &= \lim_{t \rightarrow \infty} t \text{lim} \eta^{AB}(t), \\ \eta^{AB}(t) &= \int_0^t ds \rho_{\eta}^{AB}(s), \\ \rho_{\eta}^{AB}(t) &= \frac{\beta}{V} \langle J_{\eta}^A(0) J_{\eta}^B(t) \rangle, \end{aligned} \quad (10)$$

where $A, B \in \{K, \phi\}$, $\beta = 1/k_B T$, and tlim denotes the thermodynamic limit of large system size. The microscopic currents are

$$J_\eta^A(t) = T_{xy}^A[x^N(t)] \quad (11)$$

in which \mathbf{T} is the stress tensor, having kinetic and potential contributions,

$$\mathbf{T}^K = m \sum_i \vec{u}_i \vec{u}_i, \quad (12)$$

$$\mathbf{T}^\phi = -\frac{1}{2} \sum_{\vec{v}} \sum_{i \neq j} (\vec{r}_{ij} + \vec{v}L) \frac{d\phi(\vec{r}_{ij} + \vec{v}L)}{d(\vec{r}_{ij} + \vec{v}L)},$$

in which \vec{u}_i is the velocity in the center-of-mass frame of reference,

$$\begin{aligned} \vec{u}_i &= \vec{v}_i - \vec{v}, \\ \vec{v} &= \frac{1}{N} \sum_i \vec{v}_i. \end{aligned} \quad (13)$$

Subscripts x and y refer to tensor components. We observe that the center-of-mass velocity \vec{v} is independent of the time.

In addition to the calculation of the stress autocorrelation function, we have also computed the time-dependent transport coefficients $\eta^{AB}(t)$ directly from the second of Eq. (10), by rewriting the equation in the form,

$$\eta^{AB}(t) = \frac{\beta}{V} \langle J_\eta^A(0) G_\eta^B(t) \rangle, \quad (14)$$

in which

$$G_\eta^A(t) = \int_0^t ds J_\eta^A(s). \quad (15)$$

While the G_η^A are not known functions of the phase, they can easily be evaluated numerically by including their definitions as differential equations to be integrated in addition to the equations of motion. In this way we avoid the problem of integrating the stress autocorrelation function itself to obtain the viscosity coefficient.

We also compute the self-diffusion constant,

$$\begin{aligned} D &= \lim_{t \rightarrow \infty} \text{tlim} D(t), \\ D(t) &= \int_0^t ds \rho_D(s), \\ \rho_D(t) &= \langle J_D(0) J_D(t) \rangle, \end{aligned} \quad (16)$$

in which the microscopic diffusion current is

$$J_D(t) = u_{xi}(t). \quad (17)$$

A time-dependent self-diffusion constant is also readily obtained in the form

$$\begin{aligned} D(t) &= \langle J_D(0) G_D(t) \rangle, \\ G_D(t) &= \vec{R}_i(t) - \vec{R}_i(0), \end{aligned} \quad (18)$$

in which we introduce the position \vec{R}_i of particle i in the so-called infinite-checkerboard, center-of-mass frame of reference, i.e., \vec{R}_i is the integral of \vec{u}_i .

D. Long-time behavior

It is well known that the time-correlation functions for fluid transport coefficients typically decay algebraically at long times.²²⁻²⁴ Indeed, mode-coupling theory¹¹⁻¹⁴ predicts that

$$\begin{aligned} \rho_D(t) &\sim \alpha_D t^{-3/2}, \\ \rho_\eta^{AB}(t) &\sim \alpha_\eta^{AB} t^{-3/2}, \end{aligned} \quad (19)$$

with

$$\begin{aligned} \alpha_D &= \frac{2}{3n\beta m} [4\pi(D + \nu)]^{-3/2}, \\ \alpha_\eta^{KK} &= \frac{1}{120\pi^{3/2}\beta^2} \left[\frac{7}{(2\nu)^{3/2}} + \frac{1}{\Gamma_s^{3/2}} \right], \\ \alpha_\beta^{K\phi} &= 0, \\ \alpha_\beta^{\phi\phi} &= 0, \end{aligned} \quad (20)$$

where

$$\begin{aligned} \nu &= \eta/nm, \\ \Gamma_s &= \frac{(\gamma - 1)\lambda}{nC_p} + \frac{4\nu}{3} + \frac{\xi}{nm}, \\ \gamma &= C_p/C_v, \end{aligned} \quad (21)$$

in which $n = N/V$ is the number density, λ is the thermal conductivity, ξ is the bulk viscosity, and C_p and C_v are the specific heat capacities at constant pressure and volume, respectively. Because of this slow decay, care is required in estimating the long-time limit of the $\eta^{AB}(t)$.

In addition, there is both numerical^{25,10} and theoretical^{15,16} evidence that the cross and potential contributions to the stress autocorrelation function have long-time tails which, for dense fluids, dominate the kinetic contribution out to rather larger values of the time. If indeed present, these anomalous tails could severely complicate the estimation of the viscosity coefficient.

E. Method

Our calculations combine the Monte Carlo method with the equilibrium molecular dynamics to evaluate the time-correlation functions introduced above.²⁶ The reader should consult the earlier papers for details of the analysis, especially for information on the determination of the estimates of the statistical uncertainties.

F. Reduced variables

In order to express our results in dimensionless form, we introduce the usual scales of mass, length, and time,

$$\begin{aligned} m_0 &= m, \\ l_0 &= \sigma, \\ t_0 &= \sigma(m/\epsilon)^{1/2}, \end{aligned} \quad (22)$$

We notate reduced variables by the use of an overhanging caret. The state of the system is then specified through

the reduced density and temperature,

$$\hat{n} = \frac{N\sigma^3}{V}, \quad (23)$$

$$\hat{T} = k_B T / \epsilon.$$

The values for the present calculations, $\hat{n}=0.8442$ and $\hat{T}=0.722$, specify a liquid state near the triple point of the LJ system.

The self-diffusion constant is readily obtained in reduced variables from Eqs. (16), (17), and (22),

$$D = \frac{\sigma}{\sqrt{m/\epsilon}} \hat{D}, \quad (24)$$

with the corresponding reduced autocorrelation function,

$$\rho_D(t) = \frac{\epsilon}{m} \hat{\rho}_D(t). \quad (25)$$

The viscosity coefficient is, from Eqs. (9)–(12) and (23),

$$\eta = \frac{\sqrt{m\epsilon}}{\sigma^2} \hat{\eta}, \quad (26)$$

with the corresponding reduced autocorrelation function,

$$\rho_\eta(t) = \frac{\epsilon}{\sigma^3} \hat{\rho}_\eta(t). \quad (27)$$

Observe that the relation between reduced transport coefficient and reduced autocorrelation function becomes

$$\hat{\mu}(t) = \int_0^{t/t_0} ds \hat{\rho}_\mu(st_0), \quad (28)$$

for $\mu \in \{D, \eta\}$.

G. Numerical details

Because this state point is near both the liquid-gas and the liquid-solid coexistence lines, some care is required to assure that the calculations, both the Monte Carlo and the molecular dynamics, correctly traverses the fluid region of phase space. The danger of the system becoming “locked” in an ordered region is particularly acute for the smaller values of N . Both the pressure and the self-diffusion coefficient are expected to be valuable in assessing the presence of such effects.

In order to initiate the system in the liquid, the initial configuration was taken in most cases from a preliminary run for a state which lies well into the liquid, typically $\hat{T}=1.08$ with the density $\hat{n}=0.8442$. The latter run was initiated in the fcc lattice and consisted of the usual alternate Monte Carlo and molecular-dynamic sections.²⁰ Observations of the pressure (by means of the virial) showed the rapid transition to the liquid phase.

Because of the high density, the length of the individual Monte Carlo sections consisted of several hundred attempted moves for each particle, assuring that each trajectory was virtually independent of its predecessors. For the calculation of the various time-correlation functions, the phases $x^N(t)$ at times $t=0, \omega \Delta t, 2\omega \Delta t, \dots$ (where Δt is the integration time step) were chosen as time origins, with the observation of a time-correlation function for a given trajectory then consisting of the average over all

time origins for that trajectory.

The calculation of the pressure was based on the virial, Eq. (6), using both a time average of the W_N , calculated at every time step, as well as the overall Monte Carlo average. In forming the latter average, it proved to be slightly advantageous (statistically) to average the ratios of the time-averaged values of W_N and E_k . The pressure obtained in this way was in good agreement with that based on using the exact Eq. (8) for the kinetic energy but had a somewhat smaller standard deviation. Thus the reported values of the pressure presumably contain a small but quite tolerable bias. The Verlet²⁷ “leap-frog” integration procedure was used because of its ease of use and, more importantly, because the algorithm is symplectic.

III. RESULTS

We have studied systems of 108 to 4000 LJ particles for the selected state point. In Table I are listed the parameters of the calculations, including the number of attempted Monte Carlo moves per particle between trajectories (N_{MC}), the number of trajectories (N_{tr}), number of time steps (N_{stp}), for each trajectory, each step of length Δt , typically $0.002t_0$, and the time-origin spacing ω (in time steps). The longest time t_f for which the various time-correlation functions were calculated is also given; it is roughly $1.65t_0$ in each case. Finally, we list the acoustic-wave traversal time t_a for each system,

$$t_a = L/c, \quad (29)$$

based on the sound speed $c=5.8l_0/t_0$ reported by Levesque and Verlet.⁸ Typically for time-correlation functions, finite system effects can be expected to become important for times greater than t_a .²⁶ The table includes calculations both for the cubic-spline-modified LJ poten-

TABLE I. Parameters for the Monte Carlo, molecular-dynamics calculations of the equation of state and time-correlation functions for self-diffusion and shear viscosity at reduced density 0.8442 and reduced temperature 0.722. N is the number of particles, ϕ denotes the interaction potential modification, s for cubic spline or t for the 2.5σ truncation, N_{MC} is the number of Monte Carlo moves per particle from one trajectory to the next, N_{tr} is the number of trajectories, each of N_{stp} time steps Δt , ω is the number of time steps per time origin, t_f is the largest time for which the time-correlation functions were evaluated, t_a is the acoustic-wave traversal time, and t_0 specifies the time scale, Eq. (22). The total number of time steps for a given realization is the product $N_{tr}N_{stp}$.

N	ϕ	N_{MC}	N_{tr}	N_{stp}	$\Delta t/t_0$	ω	t_f/t_0	t_a/t_0
108	s	800	300	8000	0.002	2	1.652	0.869
108	t	400	54	16 800	0.004	10	1.680	0.869
256	s	800	72	8000	0.002	2	1.652	1.158
500	s	200	108	8000	0.002	2	1.652	1.448
864	s	400	176	11 200	0.002	4	1.656	1.738
864	t	400	29	11 200	0.002	4	1.656	1.738
1372	s	400	122	8400	0.002	6	1.656	2.072
4000	s	400	104	2800	0.002	2	1.656	2.896

TABLE II. Equation of state and transport coefficient results for the Lennard-Jones liquid at reduced density 0.8442 and reduced temperature 0.722. N is the number of particles, ϕ specifies the interaction potential modification, s for the cubic spline or t for the 2.5σ truncation, f is the statistical degrees of freedom for the observed mean values: p is the pressure, V the volume, N the number of particles, k_B is Boltzmann's constant, T is the temperature, and Φ is the potential energy. The transport coefficients include \hat{D} , the reduced self-diffusion constant, $\hat{\eta}^{KK}$, $\hat{\eta}^{K\phi}$, $\hat{\eta}^{\phi\phi}$, and $\hat{\eta}$, the kinetic, cross, potential, and total reduced shear viscosity coefficients evaluated at time t_f (see Table I). Each statistical uncertainty, given in parentheses in units of the low-order digit of the mean, is 1 standard deviation of the mean.

N	ϕ	f	$pV/Nk_B T$	$\Phi/Nk_B T$	$\hat{D}(t_f)$	$\hat{\eta}^{KK}(t_f)$	$\hat{\eta}^{K\phi}(t_f)$	$\hat{\eta}^{\phi\phi}(t_f)$	$\hat{\eta}(t_f)$
108	s	96	2.687(17)	-6.1426(42)	0.0245(2)	0.048(1)	0.024(6)	3.308(63)	3.404(63)
108	t	53	1.323(51)	-7.8220(94)	0.0288(4)	0.047(1)	0.024(6)	2.816(73)	2.912(71)
256	s	71	2.855(21)	-6.1225(55)	0.0265(3)	0.048(4)	0.014(14)	3.746(170)	3.822(170)
500	s	94	2.867(15)	-6.1212(38)	0.0273(2)	0.051(2)	0.011(11)	3.693(140)	3.761(130)
864	s	87	2.874(8)	-6.1194(20)	0.0280(1)	0.052(1)	0.025(8)	3.552(79)	3.654(81)
864	t	28	1.419(29)	-7.8209(53)	0.0320(3)	0.049(3)	0.039(14)	3.074(160)	3.200(160)
1372	s	60	2.878(6)	-6.1183(16)	0.0283(1)	0.053(2)	0.033(9)	3.637(110)	3.756(110)
4000	s	103	2.867(5)	-6.1219(13)	0.0284(1)	0.049(3)	0.036(21)	3.787(270)	3.909(270)

tial as well as for the truncated LJ. For the present section we will only be concerned with the former. For each system, we have evaluated the pressure, and the time-correlation functions for self-diffusion and viscosity.

Except for the $N=108$ system, there was no evidence for the systems locking into a solid phase. During the $N=108$ run, the system appeared to spontaneously freeze for roughly nine trajectories, after which the system again became liquid. The transition to the solid was marked by a rapid decrease in both pressure and the self-diffusion constant, the latter being essentially zero for these trajectories. Because this calculation did not show any other such transitions, the overall average could not be expected to sample the solidlike region of phase space very well. Therefore, we eliminated these nine trajectories in computing the averages. Their inclusion would not have greatly affected the averages, but would lead to a pronounced increase in the statistical uncertainties, at least of the pressure and the self-diffusion constant.

A. Pressure

The observed values of the compressibility factor $pV/Nk_B T$ are listed in Table II. These are plotted as a function of $1/N$ in Fig. 1. As previously observed for high-density hard disks¹⁸ and spheres¹⁰ as well as the LJ fluid,²⁰ the pressure is not a monotonic function of N over the range of these calculations. The effect appears to least qualitatively similar in that the apparent maximum in the pressure occurs near $N=500$.

It is also noteworthy that the pressure for the present potential is much higher than $pV/Nk_B T=0.25$ reported by Levesque *et al.*¹ for their truncated (2.5σ) LJ potential, corrected (presumably) for distances beyond that. The standard correction for a potential truncated at distance r_m ,²⁷

$$\Delta \left[\frac{pV}{Nk_B T} \right] = - \frac{2\pi n}{3k_B T} \int_{r_m}^{\infty} dr r^3 \phi'(r)g(r), \quad (30)$$

yields [in the $g(r)=1$ approximation] -1.25 for $r_m=2.5\sigma$. The present potential energy function requires no tail correction, of course, but in view of the

magnitude of the full LJ correction the difference is not unexpected.

As a check that our computer calculations are correct, we generated realizations for 108 and 4000 particles for the state $\hat{n}=0.7$, $\hat{T}=2.75$, in order to compare with the results of Holian and Evans²¹ for the same interaction potential. Our compressibility factors, 3.20 ± 0.06 and 3.13 ± 0.05 , are in satisfactory agreement with theirs, 3.15 ± 0.01 and 3.11 ± 0.003 , for $N=108$ and 4000, respectively. (Note, however, that the latter are for the molecular-dynamics ensemble, rather than our NVT ensemble.)

As an additional check, we generated a 108-particle realization for $\hat{n}=0.82$, $\hat{T}=1.06$ for the truncated (2.5σ)

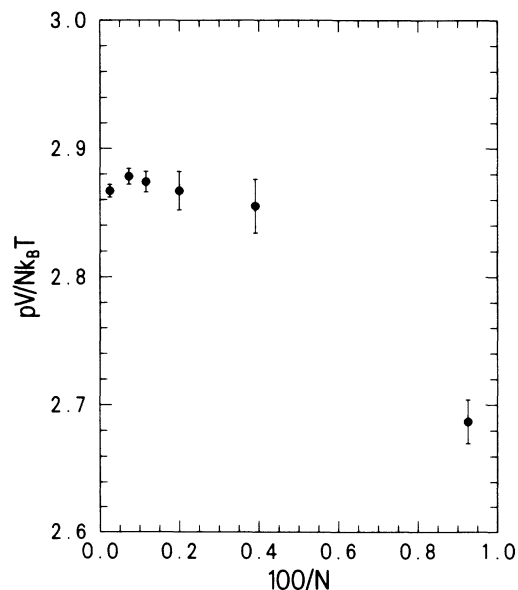


FIG. 1. Compressibility factor $pV/Nk_B T$ as a function of the inverse of number of particles N for the (cubic-spline-modified) Lennard-Jones liquid near the triple point. The error bars represent ± 1 standard deviation about the mean.

LJ potential, in order to compare with the Monte Carlo results of McDonald and Singer.²⁸ Applying the tail correction, Eq. (30), of 0.83 to our result, we compare our 1.89 ± 0.07 with their 1.82 ± 0.05 , which is quite satisfactory.

Finally, we fit our results for the compressibility factor for the four largest system sizes through linear least squares to obtain

$$\frac{pV}{Nk_B T} = 2.8639 \pm 0.0058, \quad (31)$$

for the thermodynamic limit.

B. Self-diffusion

The time-dependent self-diffusion constant, evaluated at the longest time considered, t_f , is also given in Table II and plotted against $1/N$ in Fig. 2. In contrast to our recent study²⁰ of self-diffusion at $\hat{n}=0.85$, $\hat{T}=1.08$, there is little to suggest anything other than a linear dependence on $1/N$. An estimate for the self-diffusion constant in the thermodynamic limit can be made through a linear least-squares fit to the results in Table II, yielding

$$\hat{D}(t_f) = 0.028521 \pm 0.000062. \quad (32)$$

The theoretical long-time tail, Eqs. (19) and (20), can be evaluated using the transport coefficients and heat capacities of Levesque and Verlet.⁸ Evaluated at time t_f , it is found to be quite small ($\sim 10^{-4}$), but is in statistical agreement with the observed time-correlation function, Fig. 3, which turns positive just before t_f , following a rather long negative piece which is similar to the negative

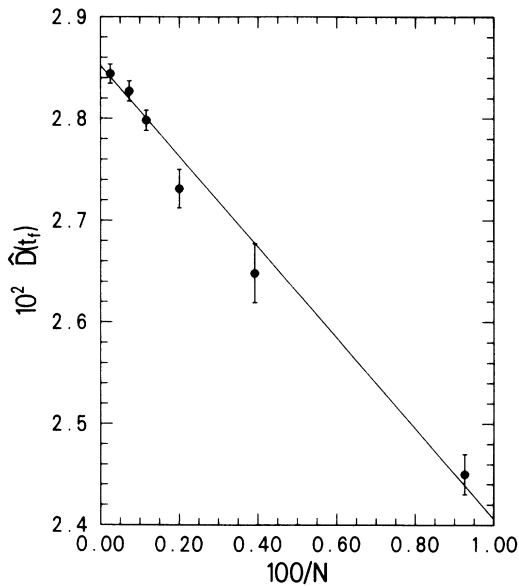


FIG. 2. Self-diffusion constant from the Green-Kubo integral out to the longest observation time t_f as a function of the inverse of the number of particles N for the (cubic-spline-modified) Lennard-Jones liquid near the triple point. The error bars represent ± 1 standard deviation about the mean. The line is the least-squares fit to the data, weighted by the inverse of the variance of the individual datum.

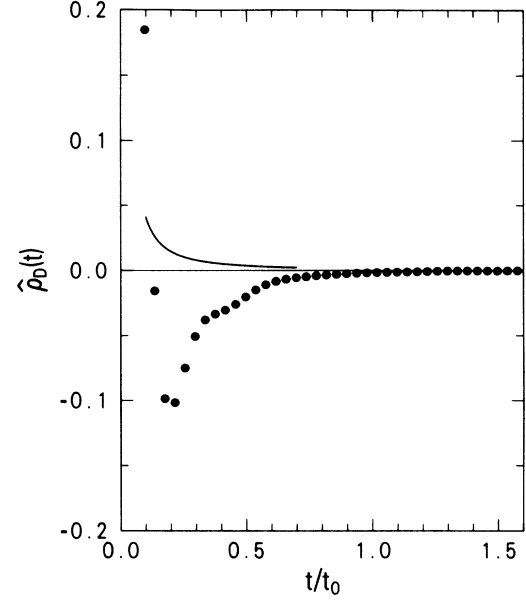


FIG. 3. Reduced autocorrelation function for self-diffusion (the velocity autocorrelation function) $\hat{\rho}_D(t)$ as a function of time t , relative to the time scale t_0 , given in Eq. (22), for a system of 4000 (cubic-spline-modified) Lennard-Jones particles near the triple point. The solid curves shows the prediction of mode-coupling theory. The error bars represent ± 1 standard deviation about the mean.

piece of the velocity autocorrelation function for hard spheres at high density.¹⁰ Therefore we add the integral of the tail to infinite time, yielding a contribution 0.001914 to \hat{D} , whence we obtain as a final estimate

$$\hat{D} = 0.030435 \pm 0.000062. \quad (33)$$

It is perhaps worth noting that, although this value is small, it is clearly positive and characteristic of a fluid.

C. Shear viscosity

Here we consider in greater detail both the time-dependent viscosity coefficients $\hat{\eta}^{AB}(t)$ and the corresponding time-correlation functions $\hat{\rho}_{\eta}^{AB}(t)$ for values of the time out to roughly $1.65t_0$. We first discuss the behavior of the time-dependent viscosity coefficients and their extrapolation to the thermodynamic limit.

1. Time-dependent viscosity coefficient

Included in Table II are the observed values of the three contributions to the $\hat{\eta}(t)$ (as well as the total shear viscosity) for the latest time for which observations were made, viz., $t = t_f$. The total viscosity $\hat{\eta}(t_f)$ is plotted against $1/N$ in Fig. 4. Clearly these results are consistent with a linear dependence of $\eta(t_f)$ on $1/N$, although the anomaly observed for the equation of state would perhaps lead one to expect a similar anomaly here. While there is perhaps some slight suggestion of that, at the current level of statistical precision a linear least-squares fit is indicated, which leads to the infinite-system result

$$\hat{\eta}(t_f) = 3.773 \pm 0.064, \quad (34)$$

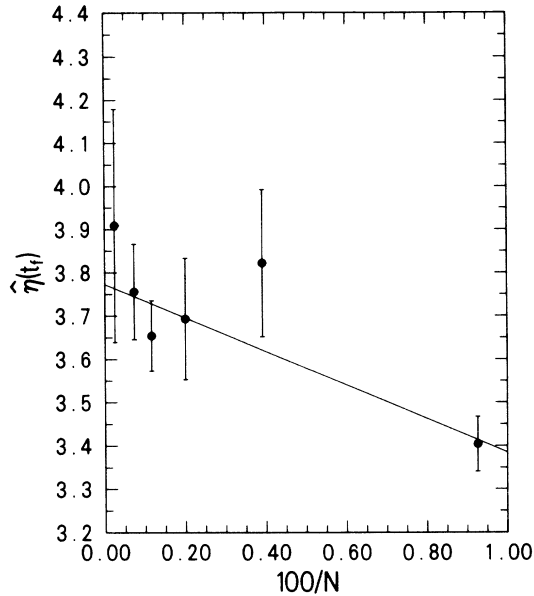


FIG. 4. Reduced shear viscosity $\hat{\eta}(t)$ from the Green-Kubo integral out to the longest observation time t_f as a function of the inverse of the number of particles N for the (cubic-spline-modified) Lennard-Jones liquid near the triple point. The error bars represent ± 1 standard deviation about the mean. The line is the least-squares fit to the data, weighted by the inverse of the variance of the individual datum.

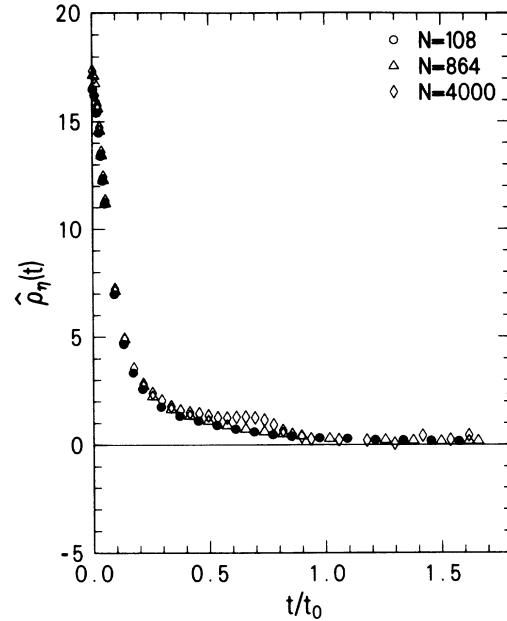


FIG. 5. Reduced shear viscosity autocorrelation function $\hat{\rho}_\eta(t)$ as a function of time t relative to the time scale t_0 , Eq. (22), for systems of 108, 864, and 4000 (cubic-spline-modified) Lennard-Jones particles near the triple point. The full range of time investigated is displayed.

with a nominal goodness-of-fit value. To extrapolate using only the $N \geq 864$ results would yield a value somewhat larger, but in statistical agreement.

Despite the small magnitude of the N dependence which we observe, it is nonetheless interesting to consider the origin of the differences in greater detail. We consider, therefore, the behavior of the ρ_η time autocorrelation function.

2. Stress autocorrelation function

In Fig. 5, we show the (total) stress autocorrelation function as a function of time for systems of 108, 864, and 4000 particles. The statistical uncertainties (one standard deviation) are smaller than the plotting symbols, so that the visible differences between the data for the various values of N are statistically significant. Nonetheless, the N dependence exhibited here is clearly not large.

The differences at small times is shown in greater detail in Fig. 6, which includes results for all six values of N . The most striking feature of the data is the apparent lack of a monotonic dependence on N . The $N=108$ curve is shifted upward for $N=256$ and 500 but sharply downward for $N=864$. Further increase in N leads to a further upward sweep of the curve toward the $N=1372$ and 4000 curves. The latter pair show no further N dependence on the scale of the figure.

Nonetheless, it is important to realize the $\hat{\rho}_\eta(t)$ data for a given N are rather strongly serially correlated over the times shown in Fig. 6, as is evident from the smoothness

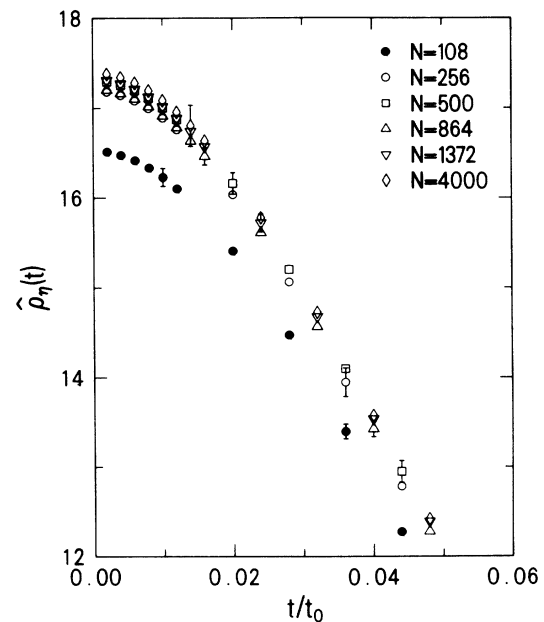


FIG. 6. Reduced shear viscosity autocorrelation function $\hat{\rho}_\eta(t)$ as a function of time t relative to the time scale t_0 , Eq. (22), for systems of 108, 256, 500, 864, 1372, and 4000 (cubic-spline-modified) Lennard-Jones particles near the triple point. Short times only are displayed. The error bars represent ± 1 standard deviation about the mean.

of the data compared to the statistical uncertainties. Therefore, while one can draw conclusions based on the error bars for a fixed value of the time, one can also be easily misled in the belief that a trend is present which is not supported by the data. To obtain an accurate appraisal of the implications of the stress autocorrelation function data at early times, we plot in Fig. 7 $\hat{\rho}_\eta$ against $1/N$ for a fixed value of the time, near the middle of the interval covered by Fig. 6. Clearly, there is little evidence that the dependence is other than monotonic.

The behavior of ρ_η at times between $0.3t_0$ and $0.9t_0$ is shown in Fig. 8. Again, there is perhaps a suggestion that the dependence on N is not monotonic, but that conclusion is not supported by the data in light of the serial correlation.

3. Long-time tail

The existence of a long-time tail for the viscosity of the triple-point LJ fluid has been a subject of conflicting evidence in the literature. In particular, Evans²⁵ reported the existence of an "enhanced" tail, based on his NEMD calculations using an oscillatory shear technique. Schoen and Hoheisel,⁹ however, concluded that no significant long-time tail exists, based on their direct (equilibrium) molecular-dynamics calculations.

In Fig. 9, we plot the long-time data for the stress autocorrelation function against $(t/t_0)^{-3/2}$ for the three systems for which our calculations are most extensive, $N=108$, 864, and 1372. For the smaller two systems, the suggestion of a $t^{-3/2}$ decay is similar to that seen for hard spheres.¹⁰ While we do not display the kinetic, cross, and potential parts separately, it is true here, just as in the hard-sphere case, that these three contributions have rather different magnitudes, with the potential con-

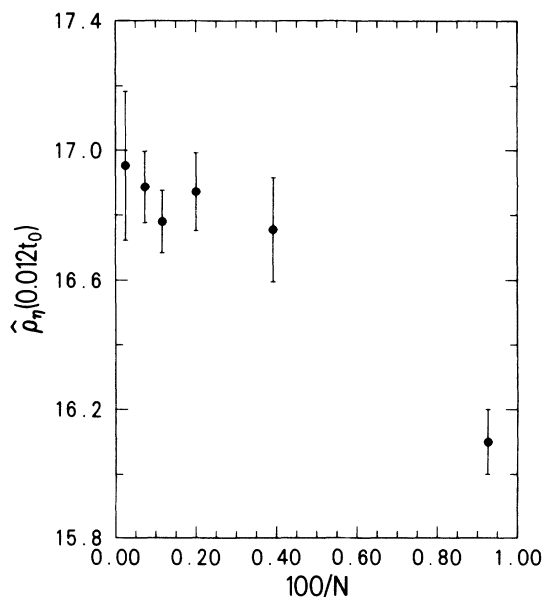


FIG. 7. Reduced shear viscosity autocorrelation function $\hat{\rho}_\eta$ for a fixed value of the time, $0.012t_0$ [t_0 is time scale, Eq. (22)] as a function of the inverse of the number of particle N . The error bars represent ± 1 standard deviation about the mean.

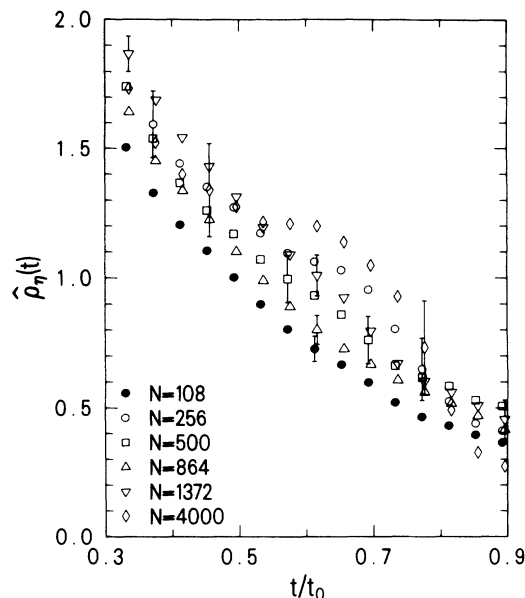


FIG. 8. Reduced shear viscosity autocorrelation function $\hat{\rho}_\eta(t)$ as a function of time t relative to the time scale t_0 , Eq. (22), for systems of 108, 256, 500, 864, 1372, and 4000 (cubic-spline-modified) Lennard-Jones particles near the triple point. Intermediate and long times only are displayed. The error bars represent ± 1 standard deviation about the mean.

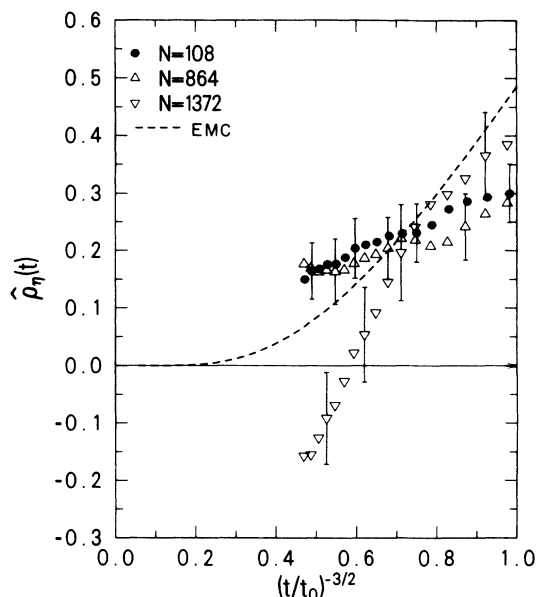


FIG. 9. Reduced shear viscosity autocorrelation function $\hat{\rho}_\eta(t)$ as a function of time t relative to the time scale t_0 , Eq. (22), for systems of 108, 864, and 1372 (cubic-spline-modified) Lennard-Jones particles near the triple point. Long-time data only is displayed. The error bars represent ± 1 standard deviation about the mean. The curve is the extended mode-coupling theory, with amplitude fitted to the 4000-particle data.

tribution dominant. The $N=1372$ data suggest a more complicated decay, with considerable dependence on the number of particles even for this rather large system and even though the time is less than the acoustic traversal time (Table I).

To compare with the predictions of simple mode-coupling theory, Eq. (19), we evaluate α_η , Eq. (20), using the transport coefficients and heat capacities of Levesque and Verlet.⁸ The resulting tail is indistinguishable from the $\rho_\eta=0$ axis in Fig. 5. At time t_f , the mode-coupling prediction

$$\hat{\rho}_\eta(t) \sim 3.17 \times 10^{-4} (t/t_0)^{-3/2} \quad (35)$$

is indeed small compared to the observed value, say, for $N=4000$, viz., $\hat{\rho}_\eta(t_f) = 0.44 \pm 0.18$. If we fit the data of Fig. 9, say, for $N=864$, to the form,

$$\hat{\rho}_\eta(t) \sim a (t/t_0)^{-3/2}, \quad (36)$$

then we find that

$$a \approx 820 \alpha_\eta^{(KK)}, \quad (37)$$

a result not unlike that found for hard spheres.¹⁰

The extended mode-coupling theory of Kirkpatrick,¹⁵ van Beijeren,¹⁶ and de Scheper *et al.*¹⁷ appears to provide quantitative agreement with the long-time stress autocorrelation function for hard spheres. We might well anticipate that similar agreement would be obtained for the LJ fluid. In order to estimate an extended mode-coupling (EMC) contribution, we proceed by using the hard-sphere form¹⁷

$$\rho_{\text{EMC}}(t) = (2\eta_E/t_\sigma) A(\hat{n}) \exp[-2z_h(k_G)t], \quad (38)$$

in which η_E is the Enskog value of the viscosity, $t_\sigma = (\beta m)^{1/2} \sigma / 2$, A is an amplitude, known in terms of the structure factor, and $z_h(k_G)$ is the extended hydrodynamic-mode eigenvalue for the heat mode, evaluated at the "de Gennes minimum," given approximately as a function of density by

$$z_h(k_G) = 4.18(1.056 - \hat{n})/t_\sigma. \quad (39)$$

To obtain our estimate, we replace the hard-sphere diameter by the Lennard-Jones σ to evaluate z_h , and obtain an empirical value for A through a least-squares fit of our 4000-particle data to Eq. (38), yielding

$$\hat{\rho}_{\text{EMC}}(t) = (9.84 \pm 1.66) \exp[-3.009t/t_0]. \quad (40)$$

This result is also plotted in Fig. 9. The resulting increment to the viscosity coefficient is

$$\begin{aligned} \Delta\hat{\eta} &= \int_{t_f/t_0}^{\infty} ds \hat{\rho}_{\text{EMC}}(s) \\ &= 0.0228 \pm 0.0038, \end{aligned} \quad (41)$$

yielding our final estimate,

$$\hat{\eta} = 3.796 \pm 0.068. \quad (42)$$

For comparison, we note that the simple mode-coupling correction is $\Delta\hat{\eta}_{\text{MC}} = 0.0008$. Again we stress that this result applies to the cubic-spline-modified LJ potential, rather than the full or truncated potentials.

IV. COMPARISON WITH PREVIOUS RESULTS

To compare with earlier work, it is necessary to estimate the effect of the different potential energy functions. For the equation of state, we have seen in Sec. III that the effect of this difference is quite substantial, but entirely in line with the magnitude expected on the basis of corrections to the virial, Eq. (30).

For the stress autocorrelation function, we are not aware of any attempt to correct for the truncation of the potential. This is true with respect to both the GK and the NEMD calculations. (In view of this neglect, it seems that the comparison of molecular dynamics (MD) results with the experimental argon viscosity coefficient is not entirely germane.) From the present point of view, however, it is important that we assess the difference between the viscosity coefficients which can be attributed to the difference in the interparticle forces. Indeed, we might also regard this difference as a measure of the difference which could reasonably be expected to arise from the truncation of the LJ potential itself.

In order to assess the effect of the details of the potential, we have repeated our calculations using the truncated (2.5σ) LJ potential for 108 and 864 particles. These realizations are also described in Table I and the major results given in Table II. In both cases, the time-dependent viscosity coefficient at time t_f is decreased for

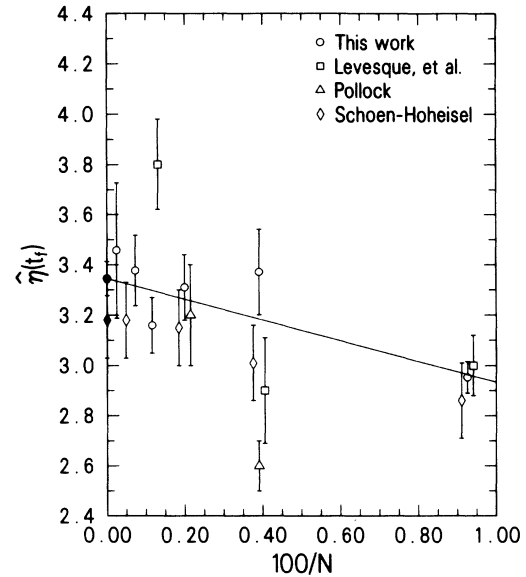


FIG. 10. Reduced shear viscosity $\hat{\eta}(t)$ from the Green-Kubo integral out to the longest observation time t_f as a function of the inverse of the number of particles N for the truncated (at 2.5σ) Lennard-Jones potential liquid near the triple point, including the present results, corrected for the difference in the interaction potential, as well as results by other authors. The closed symbols show the results of extrapolation to the thermodynamic limit. To facilitate the comparison of the results, some points have been displaced a little to the left or right. The error bars represent ± 1 standard deviation about the mean. The line is the least-squares fit of the present results.

the truncated potential, by roughly 0.5 (in reduced units) for the smaller system and 0.4 for the larger, although both changes are in statistical agreement. In lieu of any substantial dependence of this difference on system size, we chose the average of these two differences, viz., 0.451, as a crude estimate for all values of N . Applying the same correction to our estimate, Eq. (42), we obtain our estimate for the truncated potential,

$$\hat{\eta} = 3.345 \pm 0.068. \quad (43)$$

In light of this, we compare our results for $\hat{\eta}(t_f)$ with those of previous workers for various values of N in Fig. 10, including the Schoen-Hoheisel estimate $\hat{\eta} = 3.18 \pm 0.15$ for the thermodynamic limit. Only the single 864-particle results presented by Levesque and Verlet⁸ is plotted, inasmuch as it is an extension of the earlier calculation.¹

With two notable exceptions, it is evident that there is rather good agreement among the various results. In addition to the much publicized Levesque-Verlet outlier at $N=864$, the Pollock result at $N=256$ appears even more exceptional, lying 6 standard deviations from the least-squares line. In the absence of any details of the Pollock calculations, one could only speculate concerning the source of the discrepancy.

The Levesque and Verlet result for 864 particles remains something of a mystery. Their hypothesis that it represents a long-lived glassy state seems untenable in that the density is that of a liquid and the observed equation of state agrees so well with that observed in the present work. Finally, such a long-lived state has not been observed in any other study.

It is important to realize that the point is nearly 3 standard deviations removed from the least-squares line. Among the 15 data points shown in the figure, one would not expect any of them to be that far removed. The most ready explanation of this circumstance is provided by questioning the quoted statistical uncertainty. While the authors provide some detail on the calculation of statistical uncertainties, there is not sufficient detail to assure, for example, that the individual observations used to obtain averages and standard deviations are uncorrelated. The presence of such correlations would lead to underestimation of the uncertainty. Moreover, the estimation of the standard deviation by Levesque and Verlet was based on the assumption that their sample variance was independent of the number of particles. It was, then, computed from their results for 108 and 256 particles as well as for 864 particles. Our results indicate that the sample variance (for a fixed spacing of time origins) increases rather substantially with N . Again, the effect would be to underestimate the error bar for 864 particles. Even a 50% underestimation of the standard deviation would result in a deviation of not unreasonable magnitude.

The agreement between our result for the thermodynamic limit and that of Schoen and Hoheisel⁹ can also be seen in Fig. 10. The difference is not statistically significant. Because their calculations typically extend to times of $1.3t_0$, it seems likely that their calculation does not adequately account for the long-time contributions to the viscosity, particularly in that they fit their stress auto-

correlation function data with a pair of Gaussians in the time. The long-lived contributions seen, for example, in Fig. 9 would most certainly be underestimated by that procedure.

The NEMD estimate, $\hat{\eta} = 3.15 \pm 0.1$, for the viscosity coefficient, based on 108-particle calculations, is similarly in reasonable agreement with our results, both for 108 particles and for the thermodynamic limit. In view of the small dependence on N seen here, it would indeed be surprising if the NEMD calculation were to show a larger effect.

V. DISCUSSION

We close this paper by drawing the reader's attention to the following points.

(1) In the absence of a correction for the enhanced mode-coupling tail, the present value for the viscosity coefficient is similar to that of Schoen and Hoheisel. However, the small (but large compared to the simple mode-coupling tail) but significant long-time tail needs to be taken into account to complete the calculation of the viscosity.

(2) In view of the insensitivity of the viscosity coefficient to the number of particles, it is not surprising that the NEMD calculations show a similar insensitivity and that the NEMD viscosity coefficient for 108 particles is in substantial agreement with the Green-Kubo result in the thermodynamic limit. However, that agreement may well be somewhat fortuitous, inasmuch as the NEMD result is based on an extrapolation to zero shear rate using a square-root dependence which is almost certainly wrong,^{29,30} leading then to an overestimate of η . Whether NEMD, at least through the large shear-rate calculations used by Hoover, Evans, and co-workers, can actually yield an accurate value remains to be seen.

(3) It should be recognized that much of the long-standing controversy over the Green-Kubo and the NEMD calculations has arisen because of uncertainties concerning the precision of the values obtained by either method. The tendency to recognize the evaluation of the mean value as important but regarding the variance of the mean as incidental has strongly influenced the controversy discussed here.

(4) The large difference in the viscosity between the cubic-spline-modified LJ system and the truncated LJ system suggests that the correction to the truncated LJ result for the full LJ potential may also be important. The agreement of the result for the truncated potential with the experimental argon value may well be something of an accident.

ACKNOWLEDGMENTS

The author is grateful to J. D. Johnson, M. S. Shaw, and B. L. Holian of the Los Alamos National Laboratory and W. W. Wood of Carroll College for numerous discussions. The author is grateful to Debi J. Erpenbeck for her editorial suggestions on the manuscript. This work was supported by the Division of Chemical Sciences, Office of Basic Energy Sciences, U.S. Department of Energy.

- ¹D. Levesque, L. Verlet, and J. Kürkijarvi, *Phys. Rev. A* **7**, 1690 (1973).
- ²W. T. Ashurst and W. G. Hoover, *Phys. Rev. Lett.* **31**, 206 (1973).
- ³W. G. Hoover and W. T. Ashurst, in *Theoretical Chemistry: Advances and Perspectives*, edited by H. Eyring and D. Henderson (Academic, New York, 1975), pp. 1–51.
- ⁴E. M. Gosling, I. R. McDonald, and K. Singer, *Mol. Phys.* **26**, 1475 (1973).
- ⁵A. W. Lees and S. F. Edwards, *J. Phys. C* **5**, 1921 (1972).
- ⁶W. G. Hoover, D. J. Evans, R. B. Hickman, A. J. C. Ladd, and B. Moran, *Phys. Rev. A* **22**, 1690 (1980).
- ⁷D. J. Evans and G. P. Morriss, *Phys. Rev. A* **30**, 1528 (1984).
- ⁸D. Levesque and L. Verlet, *Mol. Phys.* **61**, 143 (1987).
- ⁹M. Schoen and C. Hoheisel, *Mol. Phys.* **56**, 653 (1985).
- ¹⁰J. J. Erpenbeck and W. W. Wood, *J. Stat. Phys.* **24**, 455 (1981).
- ¹¹M. H. Ernst, E. H. Hauge, and J. M. J. van Leeuwen, *Phys. Rev. Lett.* **25**, 1254 (1970).
- ¹²M. H. Ernst, E. H. Hauge, and J. M. J. van Leeuwen, *Phys. Rev. A* **4**, 2055 (1971).
- ¹³M. H. Ernst, E. H. Hauge, and J. M. J. van Leeuwen, *J. Stat. Phys.* **15**, 7 (1975).
- ¹⁴M. H. Ernst, E. H. Hauge, and J. M. J. van Leeuwen, *J. Stat. Phys.* **15**, 23 (1976).
- ¹⁵T. R. Kirkpatrick, *Phys. Rev. Lett.* **53**, 1735 (1984).
- ¹⁶H. van Beijeren, *Phys. Lett.* **105A**, 191 (1984).
- ¹⁷I. M. de Schepper, A. F. Haffmans, and H. van Beijeren, *Phys. Rev. Lett.* **57**, 1715 (1986).
- ¹⁸W. W. Wood, *J. Chem. Phys.* **52**, 729 (1970).
- ¹⁹J. J. Erpenbeck and W. W. Wood, *J. Stat. Phys.* **35**, 321 (1984).
- ²⁰J. J. Erpenbeck, *Phys. Rev. A* **35**, 218 (1987).
- ²¹B. L. Holian and D. J. Evans, *J. Chem. Phys.* **78**, 5147 (1983).
- ²²J. R. Dorfman and E. G. D. Cohen, *Phys. Rev. Lett.* **25**, 1257 (1970).
- ²³J. R. Dorfman and E. G. D. Cohen, *Phys. Rev. A* **6**, 776 (1972).
- ²⁴J. R. Dorfman and E. G. D. Cohen, *Phys. Rev. A* **12**, 292 (1975).
- ²⁵D. J. Evans, *J. Stat. Phys.* **22**, 81 (1980).
- ²⁶J. J. Erpenbeck and W. W. Wood, *Statistical Mechanics, Part B, Time Dependent Processes*, Vol. 6 of *Modern Theoretical Chemistry*, edited by B. J. Berne (Plenum, New York, 1977), p. 1.
- ²⁷L. Verlet, *Phys. Rev.* **159**, 98 (1967).
- ²⁸I. R. McDonald and K. Singer, *Mol. Phys.* **23**, 29 (1972).
- ²⁹J. J. Erpenbeck, *Phys. Rev. Lett.* **52**, 1333 (1984).
- ³⁰J. P. Ryckaert, A. Bellmans, G. Ciccotti, and G. V. Paolini, *Phys. Rev. Lett.* **60**, 128 (1988).